Published in final edited form as:
Mol Genet Metab. 2012 September ; 107(1-2): 161–172. doi:10.1016/j.ymgme.2012.07.002.

Long Circulating Enzyme Replacement Therapy Rescues Bone Pathology in Mucopolysaccharidosis VII Murine Model

Daniel J. Rowan[1,†], **Shunji Tomatsu**[2,†], **Jeffrey H. Grubb**[3,†], **Bisong Haupt**[4], **Adriana M. Montaño**[5], **Hirotaka Oikawa**[5], **Catalina Sosa**[5], **Anping Chen**[3], and **William S. Sly**[3]

[1]School of Medicine, Saint Louis University, St. Louis, Missouri, USA

[2]Departments of Biomedical Research and Orthopedic Surgery, Alfred I. duPont Hospital for Children

[3]Edward A. Doisy Department of Biochemistry and Molecular Biology, Saint Louis University, St. Louis, Missouri, USA

[4]Department of Pathology, Saint Louis University, St. Louis, Missouri, USA

[5]Department of Pediatrics, Saint Louis University, St. Louis, Missouri, USA

Abstract

Mucopolysaccharidosis (MPS) type VII is a lysosomal storage disease caused by deficiency of the lysosomal enzyme β-glucuronidase (GUS), leading to accumulation of glycosaminoglycans (GAGs). Enzyme replacement therapy (ERT) effectively clears GAG storage in the viscera. Recent studies showed that a chemically modified form of GUS (PerT-GUS), which escaped clearance by mannose 6-phosphate and mannose receptors and showed prolonged circulation, reduced CNS storage more effectively than native GUS. Clearance of storage in bone has been limited due to the avascularity of the growth plate.

To evaluate the effectiveness of long-circulating PerT-GUS in reducing the skeletal pathology, we treated MPS VII mice for 12 weeks beginning at 5 weeks of age with PerT-GUS or native GUS and used micro-CT, radiographs, and quantitative histopathological analysis for assessment of bones.

Micro-CT findings showed PerT-GUS treated mice had a significantly lower BMD. Histopathological analysis also showed reduced storage material and a more organized growth plate in PerT-GUS treated mice compared with native GUS treated mice. Long term treatment with PerT-GUS from birth up to 57 weeks also significantly improved bone lesions demonstrated by micro-CT, radiographs and quantitative histopathological assay.

In conclusion, long-circulating PerT-GUS provides a significant impact to rescue of bone lesions and CNS involvement.

Correspondence and reprints: Shunji Tomatsu, MD, PhD Professor and Director, Skeletal Dysplasia Center Biomedical Research Nemours/Alfred I. dupont Hospital for Children 1600 Rockland Rd.,Wilmington, DE. 19899-0269 Tel: 011-1-302-298-7336, FAX: 011-1-302-651-6888 stomatsu@nemours.org.
†The authors state that first three authors should be regarded as joint first authors.

Keywords

enzyme replacement therapy; micro CT; quantitative histopathological assay

1. Introduction

The mucopolysaccharidoses (MPS) are a group of lysosomal storage disorders (LSDs) that result from a deficiency of lysosomal enzymes necessary for the degradation of glycosaminoglycans (GAGs). In mucopolysaccharidosis type VII (MPS VII; Sly syndrome) the GAGs, dermatan sulfate, heparan sulfate, chondroitin 4-sulfate, and chondroitin 6-sulfate, accumulate in lysosomes in the absence of the catabolic enzyme β-glucuronidase (GUS) [1]. Around 50 different mutations in the GUS gene have been identified producing a wide range of clinical severity [2]. MPS VII is characterized by short stature, dysmorphic features, corneal clouding, hepatomegaly, skeletal abnormalities collectively referred to as dysostosis multiplex, and developmental delay. These clinical manifestations become progressively worse over time if left untreated. MPS VII patients with the most severe phenotype have hydrops fetalis prenatally and often are stillborn or survive only a few months. At the other extreme, patients with attenuated manifestations of MPS VII have survived into the fifth decade of life.

Murine models of MPS VII have characteristics similar to the human disease [3,4]. MPS VII mice show GAG storage in lysosomes of visceral organs, skeleton, and brain. They have facial dysmorphism, growth retardation, deafness, behavioral deficits, and a shortened lifespan. Radiographic analysis showed significant bone dysplasia including shortened and thick long bones, sclerosis of the calvarium, and a narrow thorax. Microscopically, the epiphyseal growth plate is hypercellular and irregular and osteoblasts in the bone marrow contain vacuoles. In addition, synovial proliferation, vacuolated synovial cells, and articular-synovial synechiae have been described.

Several LSDs have been treated with enzyme replacement therapies (ERTs), which rely on mannose 6-phosphate receptor (M6PR) or mannose receptor-mediated uptake of enzymes into target cells [5-8]. This receptor-mediated ERT strategy has been used with substantial success to treat storage in visceral organs in murine MPS VII. However, GAG storage in the central nervous system (CNS) has been resistant to clearance by ERT using conventional doses of enzyme unless begun during the newborn period [9,10]. In several disease models partial correction in some areas of the brain followed repeated injections of large doses of enzyme [11-14]. Grubb et al. recently reported that a chemically modified form of GUS, treated to make it resistant to clearance from circulation by mannose and mannose 6-phosphate receptors (PerT-GUS), showed prolonged circulation (half-life over 18 hours) and was more effective than native enzyme at clearing storage from cortical and hippocampal neurons. Higher levels of enzyme in other tissues suggested improved delivery to other organs as well [15]. The mechanism, by which PerT-GUS enzyme escapes uptake by the mannose and mannose 6-phosphate receptors, relies on chemical inactivation of its terminal sugars by treatment of sodium metaperiodate followed by borohydride reduction. How long-circulating PerT-GUS gains the entry to some cell types remains unknown.

Prior studies showed that treatment with native GUS from birth to six weeks of age reduced clinical evidence of skeletal disease even though clearance of storage from chondrocytes was not seen [9,16]. In this study, we compared the skeletal response of MPS VII mice to treatment with 12 weeks of either PerT-GUS or native GUS ERT. We also assessed the skeletal effects of long-term treatment of MPS VII mouse models with PerT-GUS ERT.

Micro-CT, radiographs, and quantitative histopathology were used in parallel to define the bone pathology in MPS VII mice and their response to treatments.

2. Materials and Methods

2.1 MPS VII Tolerant Mouse

A tolerant mouse model for MPS VII [4] was developed from the original Birkenmeir GUS deficient mouse ($gus^{mps/mps}$) [17] and has been used for evaluation of the effectiveness of a variety of experimental treatments [11,15,18-20]. This mouse has characteristics similar to humans with MPS VII including a shortened face, facial dysmorphism, growth retardation, deafness, shortened lifespan, and behavioral deficits. In addition, it is immunotolerant to administered human GUS.

2.2 Purification of GUS

GUS was purified by a multistep procedure with conventional column chromatography as described [15]. Purified enzyme was frozen at -80°C where it was stable indefinitely until thawed for treatment with periodate.

2.3 Treatment of GUS with Periodate and Borohydride

The M6P and mannose recognition sites on GUS are contained in the oligosaccharide side chains of the enzyme. To inactivate the exposed carbohydrates, the enzyme was treated with sodium metaperiodate followed by sodium borohydride [15]. At the final step, the enzyme was dialyzed against two changes of 20 mM sodium phosphate, 100 mM NaCl (pH 7.5) at 4°C, and was stable when stored in this buffer at 4°C before use.

2.4 Comparison of Response to Treatment of MPS VII Mice with Native GUS and PerT-GUS

MPS VII mice were treated IV with 2 mg/kg native GUS (n=4) or PerT-GUS (n=4) for 12 weeks beginning at 5 weeks of age. One week after the last treatment, mice were euthanized and tissues were treated using the protocol described below for long-term treatment with PerT-GUS.

2.5 Long-Term Treatment of MPS VII Mice with PerT-GUS Intraperitoneally

MPS VII mice were treated from birth to six weeks with IP infusions of PerT-GUS (2 mg/kg body weight). After 6 weeks of age, mice received 2 mg/kg of the enzyme IP every other week for 27-57 weeks. One week after the last infusion, tissues from untreated ($n = 4$) or 2 mg/kg PerT-GUS treated MPS VII mice ($n = 5$; ages 27, 38, 41, 57, and 57 weeks old) were perfused at necropsy with 25 mM Tris and 140 mM NaCl (pH 7.2), fixed in 2% paraformaldehyde and 4% glutaraldehyde, postfixed in osmium tetroxide, and embedded in Spurr resin. For evaluation of lysosomal storage, toluidine blue-stained 0.5-μm-thick sections of knee joints were assessed by light microscopy. We also euthanized untreated MPS VII mice at 1 day old and ages 2.5, 5, 10, 23, 29, 32, and 36 weeks old and age-matched wild-type mice to understand the progression of the disease.

2.6 Micro-CT Analysis and Radiography

Mice were euthanized using CO_2. At dissection, leg bones, spines, and ribs were placed in 95% ethanol. A micro-CT scan was performed on each bone using a Scanco μCT40 system (Scanco Medical; Brüttisellen, Switzerland) according to manufacturer's instructions [21]. Scans were focused on cervical vertebrae 1 and 2 and the knee joint. The bones were then fixed in formalin in preparation for the micro-CT imaging, which was performed on a micro-CT scanner at 16-μm isotropic voxel size, with 250 projections, integration time of 300 msec, photon energy of 50 keV, and current of 160 μA. A three dimensional

reconstruction of each bone was made and the bone mineral density (BMD) of each knee joint was measured. Radiographs were also done for each leg, spine, and ribcage and compared. Leg measurements were recorded using plain radiographs (Supplemental Fig. 1). Measurements were recorded on mice older than 10 weeks, and the mean length measurement and standard deviation were calculated.

2.7 Quantitative Analysis of Histopathology

Cartilage thickness—The thickness of the tibia growth plate or articular cartilage was measured at five different places and averaged. This average for each mouse was then used to calculate the mean cartilage thickness for wild-type, untreated MPS VII, GUS treated MPS VII, and PerTGUS-treated MPS VII groups.

Cellularity—The number of cells in three predetermined areas of equal size in the tibia growth plate proliferative zone and articular cartilage were counted and averaged. The values reported are means and standard deviations of the average cellularity for the mice in each group.

Cell Area—Cells in the proliferative zone of tibia growth plate and articular cartilage were outlined as shown in Supplemental Figure 2 and ImageJ (National Institutes of Health, Bethesda, MD) was used to calculate the area within the outlined area. An average cell area was calculated for the proliferative zone of the growth plate and articular cartilage for each mouse. Areas reported are means with standard deviations of the average area for each mouse group.

Cells/Column—The number of cells stacked in columns perpendicular to the long axis of the tibia growth plate was counted, and the mean value was reported.

Perimeter/Length Ratio—The length and perimeter of the tibia growth plate region were measured as shown in Supplemental Figure 3 [22]. The values reported are means and standard deviations for each mouse group.

2.8 Rationale of Experimental Design

In prior experiments which compared the CNS response to GUS and PerT-GUS ERT, we used a 12 week regimen of weekly infusions and euthanized mice one week after the last infusion for examination of the storage in brain [15]. In order to compare response in bone, we used a similar regimen administering 2 mg/kg of native GUS and PerT-GUS IV. In prior studies of the response, treatment of MPS VII from birth with IV native GUS enzyme was shown to improve growth, fertility, longevity, and histology of visceral organs. However, the response of bone (chondrocytes) to ERT was limited even if treatment began at birth [9,11,16].

In experiments described elsewhere, we observed that many responses to IP PerT-GUS were equivalent to those observed in IV injections. In addition, despite the fact that PerT-GUS was taken up poorly by peritoneal lining cells, IP infused enzyme reached the same concentrations in the blood as IV infused PerT-GUS, with a 30-60 minute delay. For these reasons, we carried out a long-term treatment experiment using IP delivered PerT-GUS to see whether the results in bone compared favorably with those described in earlier trials from birth with native enzyme.

3. Results

3.1 GUS and PerT-GUS ERT Treatment of MPS VII Mice

3.1.1 Growth Plate and Articular Cartilage Histology

Growth Plate: The resting, proliferative, and hypertrophic zones of the growth plates in GUS and PerT-GUS treated mice contained enlarged and vacuolated cells (Fig. 1). Resting and proliferative zonal chondrocytes appeared larger in size in GUS treated mice compared with PerT-GUS treated mice. The growth plate was thicker and less organized in GUS mice. The normal columnar structure of the proliferative zone was also better preserved in PerT-GUS treated mice compared with GUS treated mice.

Articular Cartilage: Cells of the articular cartilage and meniscus were enlarged and vacuolated in both GUS and PerT-GUS treated mice. The articular cartilage chondrocytes were moderately smaller in PerT-GUS treated mice than in GUS treated mice. Cells in the meniscus of PerT-GUS treated mice contained noticeably less storage material compared with meniscal chondrocytes in GUS treated mice.

3.1.2 Quantitative Histopathological Analysis—To assess the morphology of the growth plate and articular cartilage in GUS and PerT-GUS treated MPS VII mice, we measured the thickness of the cartilage layer in the growth plate and articular cartilage, the cellularity in the articular cartilage and proliferative zone of the growth plate, a cross-sectional area of chondrocytes in the articular cartilage and proliferative zone of the growth plate as an estimate of cell volume, the mean number of cells aligned in columns perpendicular to the growth plate, and the ratio of the perimeter of the growth plate to its length as an indication of the amount of irregularity in the morphology of the growth plate (Supplemental Figs. 2 and 3).

These measurements supported our histological observations. The thickness of the articular cartilage in GUS and PerT-GUS treated mice was similar, however the growth plates in GUS treated MPS VII mice showed a trend towards increased thickness compared with PerT-GUS treated mice ($p = 0.51$; Fig. 2A). The cellularity of the articular cartilage and growth plate was similar in GUS and PerT-GUS treated mice (Fig. 2B). Cross sectional cell area was lower in the proliferative zone of the growth plate ($p < 0.05$) of PerT-GUS treated mice compared with GUS treated mice. Cross sectional cell area in articular cartilage chondrocytes was also lower in PerT-GUS treated mice compared with GUS treated mice, however this difference did not reach statistical significance (Fig. 2C). Two quantitative measures of growth plate organization (cells/column and growth plate perimeter/length ratio) showed that the growth plate of PerT-GUS treated mice is significantly more organized than that of GUS treated mice. The mean number of cells per proliferative zone column was higher in PerT-GUS treated mice ($p < 0.05$; Fig. 2D) and the growth plate perimeter/length ratio was lower in PerT-GUS treated mice compared with GUS treated mice ($p< 0.05$; Fig. 2E).

3.1.3 Micro-CT and Radiographic Findings—Micro-CT analysis of the bones of the knee joint and spine (Fig. 3) of GUS and PerT-GUS treated MPS VII mice showed that both GUS and PerT-GUS treatments significantly reduced the exophytic bone formation and cortical bone thickening which is seen in untreated MPS VII mice. Micro-CT scans also provided the (BMD) of the bones of the knee joint. GUS treated mice had a mean BMD of 459.11 ± 9.59 mgHA/ml, PerT-GUS treated mice had a significantly lower BMD 444.86 mgHA/ml ($p < 0.05$). This reduced BMD is evident in leg X-rays of GUS and PerT-GUS treated MPS VII mice (Fig. 4). Measurement of the thickness of the femur at its midpoint showed that the femurs of GUS treated mice remained abnormally thick (1.25 ± 0.29 mm)

compared with the femurs of PerT-GUS treated mice (1.13 ± 0.25 mm; $p < 0.05$). However, tibia length is similar in both GUS (1.60 ± 0.04 cm) and PerT-GUS (1.63 ± 0.03 cm) treated mice.

3.2 Skeletal Effects of Long-Term Treatment with PerT-GUS

3.2.1 Micro-CT Findings—Micro-CT analysis of the bones of the knee joint and spine (Fig. 5) in untreated MPS VII mice showed progressive abnormalities with age.

Knee joints: At 5 weeks of age, bones in the knee joints of untreated MPS VII mice had modest changes from those of wild-type: 1) less ossified bone, and 2) reduced amounts of trabecular bone (Fig. 5). By 23 weeks of age, the differences in the knee joints were marked. The cortical bone of the tibia and femur were thickened and abnormal periosteal bone formations were observed on the articular surfaces of the tibia and femur. The abnormalities were even more severe in 36 week-old mice (Fig. 5). Micro-CT scans also allowed BMD of mouse knees to be measured. The mean BMD of WT mice over 10 weeks-old was 496.2 ± 38.8 mgHA/mL ($n = 14$) and the mean BMD for untreated MPS VII mice ($n = 4$) was 568.5 ± 66.5 mgHA/mL, which is significantly elevated compared with WT mice ($p < 0.05$).

Treatment effects: PerT-GUS treated MPS VII mice showed marked improvements of the knee joint when compared with those of untreated MPS VII mice. Thicknesses of cortical bone of the femur and tibia were normalized and there were fewer periosteal bone formations, although the knee joints were still distinguishable from wild-type mouse knee joints (Fig. 5). Treatment reduced BMD to 499.7 ± 34.2 mgHA/mL ($n = 5$; $p = 0.08$, compared with untreated MPS VII mice).

Cervical spine: At 5 weeks of age, the vertebrae of untreated MPS VII mice appeared to have less ossified bone than those of the wild-type mice (Fig. 5). By 23 weeks of age, the vertebral arches were abnormally thickened and periosteal bone formation was seen on the transverse processes of the vertebrae. The vertebral bodies were flattened and wider (platyspondyly) than those in wild-type mice. In addition, the enlarged vertebrae encroached on the spinal canal causing spinal canal narrowing. These findings were even more prominent in 36-week-old untreated mice.

Treatment effects: A micro-CT scan ($n = 1$) of the spine of a 38-week-old treated MPS VII mouse showed less abnormal thickening of the bone than in untreated MPS VII mice ($n = 4$), resulting in less spinal canal narrowing. In addition, the vertebral bodies were not abnormally wide like those in untreated MPS VII mice (Fig. 5). Only one cervical spine from a PerT-GUS long-term therapy mouse was available for micro-CT study due to dissection-related damage to CV1-2 on the other specimens.

3.2.2 Radiographic Analysis—Radiographs comparing the lower extremities of wild-type, untreated MPS VII, and PerT-GUS-treated MPS VII mice are presented in Figure 6A. The tibias of MPS VII mice older than 10 weeks were shortened (1.54 ± 0.09 mm) when compared with those of wild-type mice (1.88 ± 0.03 mm; $p < 0.05$) (Fig. 6B). The long bones were also broad and sclerotic at 36 weeks of age when compared with those of wild-type mice. The ribcage was narrow with short and thick ribs. The sternal ends of the ribs showed decreased radiodensity on plain radiographs. The cervical vertebrae showed severely increased radiodensity when compared with those in wild-type mice.

Treatment effects: The tibia length of treated MPS VII mice (1.73 ± 0.03 cm) was significantly increased compared with untreated MPS VII mice (1.54 ± 0.09 cm, $p < 0.05$). In addition, the ribs of treated mice were longer and had significantly reduced radiodensity

compared with those of untreated mice. The cervical vertebrae of treated MPS VII mice had significantly reduced radiodensity compared with those in untreated mice (Fig. 6A).

3.2.3 Histopathologic Analysis of Knee Joints

Untreated MPS VII Mice

Articular cartilage: The knee joints of affected mice showed noticeable lysosomal storage within the articular cartilage even in the newborn mouse (day 1 or 2). Most articular chondrocytes had vacuoles, although the structure was organized (Supplemental Fig. 4). Affected mice showed marked lysosomal storage within the articular cartilage by 2.5 weeks of age. The articular cartilage layers (tangential, transitional and radial layers) were abnormally thickened. The chondrocytes were increased in number and ballooned with vacuoles although all three layers were still distinguishable and organized. The 10-week-old affected mice showed abnormal proliferation of the meniscal fibro-cartilage with ballooned vacuolated cells. The articular cartilage layers were slightly irregular and hypercellular, and chondrocytes were enlarged and vacuolated. The three layers were thinner compared with those seen at 2.5 weeks, and their structure was disorganized. The articular cartilage layers at 32 weeks of age showed more disorganization with almost complete loss of the normal arrangement of cells (Fig. 7). The surface of articular cartilage was irregular, and few chondrocytes in the tangential layer were observed. The transitional and radial layers showed hypercellularity compared with those in the age-matched wild-type mice. There were articular-meniscal-synovial fusions with marked abnormal proliferation of articular and meniscal cartilage, with thickened and vacuolated cells in the meniscus and synovium. The synovial space was markedly diminished. All articular cartilage cells showed marked distention, producing a thicker layer. The cells in the periosteum also had marked vacuolar distension.

Growth plate: The growth plate region in 1- or 2-day-old MPS VII mice had ballooned vacuolated chondrocytes in resting and proliferative zones. By 2.5 weeks of age, the growth plate was thickened but showed normal resting and proliferative zonal organization (Supplemental Fig. 4). The cells were swollen with increased fibrillary or vacuolar contents, which were especially prominent in the resting zone. The hypertrophic zone, although hypercellular, showed disorganization with a distorted arrangement of cells. The primary calcification zone was also increased in size. The longitudinal arrangement of the primary trabeculae was abnormal with the trabeculae increased in number and thickness and contained a marked increase of cartilage. Osteoblasts appeared to be increased in number, especially in the proximal intertrabecular spaces, and contained numerous vacuoles.

At 10 weeks of age, the growth plates were thicker and their boundaries became irregular. The column structure through all layers of the growth plate was disorganized. The chondrocytes were ballooned with vacuoles. The osteoblasts surrounding diaphyseal bone trabeculae and the cells lining bone marrow sinusoids contained a large amount of clear cytoplasmic vacuoles (data not shown).

At 32 weeks of age, the column structure through all layers of the growth plate was markedly disorganized and all chondrocytes were prominently ballooned with vacuoles (Fig. 7). The growth plates had a marked decrease in the number of cells in the proliferating zone. The storage was marked, with lysosomal distention in osteoblasts lining the cortical and trabecular bone and in the sinus-lining cells in the bone marrow. The light microscopic views revealed a loss of the parallel order of the bone matrix with loss of the concentric arrangement of lamellae or haversian system formation. The cortex was markedly thickened in affected mice. The osteocytes showed clearly increased cytoplasmic volumes filled with vacuoles.

PerT-GUS Treated MPS VII Mice: PerT-GUS treatment from birth to older than 6 months provided substantial improvement in bone pathology. The articular cartilage region showed reduced cellularity and improvement in irregular articular surfaces, although reduction of storage materials in chondrocytes was limited at all cartilage layers. Marked improvement was observed in the abnormal proliferation of articular and meniscal cartilage, leading to reduced articular-meniscal-synovial fusion (Fig. 7). Ligaments and connective tissues surrounding the articular cartilage in treated mice had fewer storage vesicles.

The growth plate region in treated mice showed the following: 1) improvement of architecture by reduction of thickened cartilage layer and irregular surface, and 2) reduced cell area in the proliferative zone, although vacuolated chondrocytes with lysosomal distension remained obvious (Fig. 7). Treated mice had reduced storage materials in bone marrow and restoration of bone architecture. The amount of lysosomal storage vesicles in osteoblasts was markedly reduced. The sinus lining cells in bone marrow and bone marrow cells showed complete clearance of storage vesicles. The osteocytes within the bone had substantially reduced storage material with recovery of cortical bone architecture. These pathological improvements correlated with marked improvements shown on X-ray images.

3.2.4 Quantitative Analysis of Histopathology—Quantitative analysis of the histopathology of wild-type and untreated and treated MPS VII mouse knees was carried out using the same methods described for the comparison of GUS and PerT-GUS treated mice. These measurements supported our histopathological observations. Untreated MPS VII mice ($n = 4$) had thicker growth plates ($p < 0.005$) and articular cartilage ($p < 0.02$) compared with those in wild-type mice ($n = 5$). PerT-GUS treatment ($n = 5$) reduced the thickness of both the growth plate ($p = 0.14$) and articular cartilage ($p = 0.24$) compared with those in the untreated MPS VII mice (Fig. 8A).

The articular cartilage cellularity in untreated MPS VII mice was increased ($p < 0.001$) compared with that in wild-type mice and was significantly reduced by PerT-GUS treatment ($p < 0.03$; Fig. 8B). By contrast, the cellularity in the proliferative zone of growth plate was not different statistically between wild-type, untreated MPS VII, and PerT-GUS-treated mice (Fig. 8C). Cell sizes in the growth plate and articular cartilage were greatly increased in untreated MPS VII mice compared with wild-type mice (growth plate, $p < 0.001$; articular cartilage, $p < 0.001$). PerT-GUS treatment caused a reduction in cell size at the growth plate ($p < 0.001$) and articular cartilage ($p < 0.03$; Fig. 8D). The number of cells/column in the growth plate of MPS VII mice was decreased when compared with wild-type mice ($p < 0.02$) and there was no difference when compared with PerT-GUS treatment ($p = 0.19$; Fig. 8E). The perimeter-to-length ratio of the growth plate in MPS VII mice was elevated when compared with wild-type mice ($p < 0.001$), showing the irregular morphology of the growth plate in untreated MPS VII mice. The perimeter to length ratio was reduced and approached normal in the PerT-GUS-treated mice ($p < 0.001$; Fig. 8F).

4. Discussion

This study had three main aims: 1) to compare the effectiveness of native GUS and PerT-GUS ERT and on bones in a murine model of MPS VII, 2) to evaluate the effectiveness of long-term treatment with PerT-GUS ERT on bones in MPS VII mice, and 3) to characterize the developmental skeletal pathology of untreated MPS VII mice with age using micro-CT of knee joints and cervical spine, radiography, and histopathology with quantitative analysis. Although there have been several reports on the bone pathology of MPS VII using light or electron microscopy and radiographs[9,10,16,23], this is the first analysis of bone pathology in MPS VII using micro-CT. Micro-CT can assess the three-dimensional bone structure and provide an objective measure of BMD. Quantitative histopathological analyses can also

provide objective measurements of severity in bone lesions at the cellular level. We used these two techniques to compare GUS and PerT-GUS ERT and to study the progression of bone dysplasia in untreated MPS VII mice up to 36 weeks of age, which is the normal lifespan of untreated MPS VII mice.

One of the limitations of ERT for LSDs has been the inability to correct bone pathology because of the avascularity of the growth plate unless treatment is begun in newborn period [9,16,24]. Given the effectiveness of PerT-GUS therapy in the CNS by the greatly prolonged blood clearance, the question of whether PerT-GUS treatment also works to improve bone pathology and clear skeletal GAG storage was of great interest. In the short term experiments (in which mice were treated with intravenous (IV) ERT therapy since 5 weeks old) several quantitative measurements of histopathology showed significant improvement in mice treated with PerT-GUS compared with native GUS treatment. Micro-CT studies showed greater reduction in BMD with PerT-GUS treatment which was also evident in X-rays and reduced femur thickness.

In work to be presented elsewhere, PerT-GUS was nearly as effective if given IP as if given IV (this contrasts with earlier observations with native enzyme which was much less effective if given IP because much of the delivered dose was taken up by peritoneal lining cells and never reached the circulation) (Grubb and Sly unpublished observation). Mice treated from birth to six weeks with 2 mg/kg PerT-GUS IP and then treated biweekly with the same dose showed improved growth, normal fertility, and lived beyond one year (data not published). This was the treatment paradigm used in this study.

We performed a direct comparison of the skeletal effects of ERT using native GUS or PerT-GUS in MPS VII mouse models. Micro-CT showed that both GUS and PerT-GUS treated mice had only minor exophytic bone formation and minimal cortical bone thickening, as seen in the mice treated with long-term PerT-GUS therapy. We also showed that treatment with PerT-GUS reduced BMD to a significantly lower level than GUS treatment. These findings were supported by the X-ray findings of lower radiodensity in PerT-GUS treated mouse legs than those of GUS treated mice.

We have also demonstrated here that MPS VII mice treated with IP injected PerT-GUS from birth had substantial correction of bone pathology seen on micro-CT and radiographs. Our results show that PerT-GUS treatment from birth to more than 6 months of age reduced cortical bone thickening and reduced the amount of shortening seen in long bones of the leg. In addition, PerT-GUS reduced exophytic bone formation, diminished spinal stenosis, and normalized radiodensity of the cervical spine and ribs in the MPS VII mice. The BMD of PerT-GUS treated MPS VII mice was reduced to the level of wild-type mice, however this was not a statistically significant reduction. Thus, IP injected PerT-GUS treatment addresses major components of the dysostosis multiplex associated with MPS VII.

The micro-CT and X-ray findings described here are in substantial agreement with those of Vogler et al., who reported that the joints of large limbs of weanling and older MPS VII mice had synovial proliferation with occasional villous projections and vacuolated synovial cells and showed occasional articular-synovial synechiae with hypercellular articular cartilage [3]. Similar bone proliferation in joints and tendons was observed in 39- to 40-week-old MPS II mice [25]. Severe periosteal bone formation was seen at the lateral aspect of the distal tibia in the MPS II murine model. Simonaro et al. showed that the mechanism of such abnormal bone proliferation is caused by elevated expression of inflammatory molecules in MPS diseases, which causes enhanced proliferation of cells in the connective tissue [26]. We described decreased bone formation in young MPS VII mice compared with wild-type mice, which may also be explained by the findings of Simonaro et al., that

osteoclast activity is increased due to overexpression of RANKL which is caused by the presence of increased inflammatory cytokines [26].

Another recent study [27] of the mechanism of bone shortening in MPS VII mice showed that growth plates had a marked decrease in the number of cells in the proliferating zone at age 3 weeks. Metcalf et al. concluded that the reduction in chondrocyte proliferation in the growth plate results in less ossification and shorter bones [27], which is consistent with our findings by micro-CT in 5-week-old MPS VII mice. These observations contrast with those reported by Vogler et al. in 3-month-old MPS VII mice in which hypercellularity of chondrocytes was seen in the growth plate [3]. The basis for these divergent observations is not yet clear.

The direct comparison of native GUS and PerT-GUS confirmed that PerT-GUS treated mice have significantly reduced storage material at the growth plate and while not statistically significant, storage material was also reduced in the articular cartilage, as indicated by cell area measurements (Fig. 2C). In addition, we show that the growth plate is less disorganized in PerT-GUS treated mice, compared with GUS treated mice as indicated by an increase in number of cells per growth plate column (Fig. 2D) and a perimeter/length ratio (Fig. 2E) which is significantly reduced towards normal in PerT-GUS treated mice. Our quantitative histological analysis showed that long-term IP injected PerT-GUS ERT improves epiphyseal growth plate organization and GAG storage and reduces growth plate thickness, cell size of chondrocytes, perimeter/length ratio of growth plate, and abnormal proliferation of articular and meniscal cartilage and connective tissue in knee joints. Previous reports on MPS VII and other types of MPS mouse models also showed clinical improvements of skeletal disease if treated with native enzyme from birth. However, chondrocytes were refractory [9,16,28]. This study with PerT-GUS showed significant reduction in size of chondrocytes (both articular and epiphyseal chondrocytes, which were half of the size of untreated chondrocytes: Fig. 8D).

It may be possible to achieve even better correction of GAG storage and pathology using a larger dose of PerT-GUS, using weekly instead of biweekly administration, or using a specifically bone-targeted form of the enzyme, which has been shown to enhance delivery to bone [24,29,30]. Even without further improvements, the results presented here suggest that PerT-GUS treatment, which has been shown to correct CNS storage in MPS VII mice, prevents skeletal pathology to a greater extent than treatment with native GUS enzyme. If similar results could be achieved in humans with MPS VII, ERT with PerT-GUS may reduce the need for corrective surgeries and improve the quality of life in MPS VII patients.

An open question is the mechanism by which Pert-GUS is taken up by the cells that show correction of storage. One possibility is that long-circulating enzyme is slowly delivered to targeted cells by non-specific fluid phase pinocytosis involving no requirements for cell surface binding. Alternatively, Pert-GUS may bind glucuronide residues of heparan sulfate in the cell surface and be slowly taken up with the internalized membrane during membrane recycling. Another mechanism by which PerT-GUS might correct bone pathology indirectly is by correcting storage in visceral macrophages that elaborate inflammatory cytokines like TNF-α. In this context, Simonaro et al. recently reported that an antibody to TNF-α could substantially reduce the skeletal pathology of rats with MPS VI [31].

In conclusion, Pert-GUS ERT provides a significant impact to rescue of the bone lesions as well as CNS involvement. This therapy could be applicable to other LSDs causing bone and brain lesions.

Supplementary Material

Refer to Web version on PubMed Central for supplementary material.

Acknowledgments

This work was supported by grants from the Austrian Research Society for Mucopolysaccharidoses and Related Diseases, Austrian MPS Society, and International Morquio Organization (Carol Ann Foundation). W.S.S. and J.H.G. were also supported by National Institutes of Health grant GM34182. The content of the article has not been influenced by the sponsors. Editorial assistance to the manuscript was provided by Michelle Stofa at Nemours/Alfred I. duPont Hospital for Children.

References

1. Neufeld, EF.; Muenzer, J. The mucopolysaccharidoses. In: Scriver, CR.; Beaudet, AI.; Sly, WS.; Valle, D., editors. Metabolic and Molecular Basis of Inherited Disease. McGraw-Hill; New York: 2001. p. 3421-3452.
2. Tomatsu S, Montaño AM, Dung VC, Grubb JH, Sly WS. Mutations and polymorphisms in GUSB gene in mucopolysaccharidosis VII (Sly Syndrome). Hum. Mutat. 2009; 30:511–519. [PubMed: 19224584]
3. Vogler C, Birkenmeier EH, Sly WS, Levy B, Pegors C, Kyle JW, Beamer WG. A murine model of mucopolysaccharidosis VII. Gross and microscopic findings in beta-glucuronidase-deficient mice. Am. J. Pathol. 1990; 136:207–217. [PubMed: 2105058]
4. Sly WS, Vogler C, Grubb JH, Zhou M, Jiang J, Zhou XY, Tomatsu S, Bi Y, Snella EM. Active site mutant transgene confers tolerance to human beta-glucuronidase without affecting the phenotype of MPS VII mice. Proc. Natl. Acad. Sci. U.S.A. 2001; 98:2205–2210. [PubMed: 11226217]
5. Barton NW, Furbish FS, Murray GJ, Garfield M, Brady RO. Therapeutic response to intravenous infusions of glucocerebrosidase in a patient with Gaucher disease. Proc. Natl. Acad. Sci. U.S.A. 1990; 87:1913–1916. [PubMed: 2308952]
6. Winkel LP, Van den Hout JM, Kamphoven JH, Disseldorp JA, Remmerswaal M, Arts WF, Loonen MC, Vulto AG, Van Doorn PA, De Jong G, Hop W, Smit GP, Shapira SK, Boer MA, van Diggelen OP, Reuser AJ, Van der Ploeg AT. Enzyme replacement therapy in late-onset Pompe's disease: a three-year follow-up. Ann. Neurol. 2004; 55:495–502. [PubMed: 15048888]
7. Rohrbach M, Clarke JT. Treatment of lysosomal storage disorders: progress with enzyme replacement therapy. Drugs. 2007; 67:2697–2716. [PubMed: 18062719]
8. Lachmann R. Treatments for lysosomal storage disorders. Biochem. Soc. Trans. 2010; 38:1465–1468. [PubMed: 21118108]
9. Vogler C, Sands MS, Levy B, Galvin N, Birkenmeier EH, Sly WS. Enzyme replacement with recombinant beta-glucuronidase in murine mucopolysaccharidosis type VII: impact of therapy during the first six weeks of life on subsequent lysosomal storage, growth, and survival. Pediatr. Res. 1996; 39:1050–1054. [PubMed: 8725268]
10. Vogler C, Sands MS, Galvin N, Levy B, Thorpe C, Barker J, Sly WS. Murine mucopolysaccharidosis type VII: the impact of therapies on the clinical course and pathology in a murine model of lysosomal storage disease. J. Inherit. Metab. Dis. 1998; 21:575–586. [PubMed: 9728337]
11. Vogler C, Levy B, Grubb JH, Galvin N, Tan Y, Kakkis E, Pavloff N, Sly WS. Overcoming the blood-brain barrier with high-dose enzyme replacement therapy in murine mucopolysaccharidosis VII. Proc. Natl. Acad. Sci. U.S.A. 2005; 102:14777–14782. [PubMed: 16162667]
12. Dunder U, Kaartinen V, Valtonen P, Väänänen E, Kosma VM, Heisterkamp N, Groffen J, Mononen I. Enzyme replacement therapy in a mouse model of aspartylglycosaminuria. FASEB J. 2000; 14:361–367. [PubMed: 10657992]
13. Roces DP, Lüllmann-Rauch R, Peng J, Balducci C, Andersson C, Tollersrud O, Fogh J, Orlacchio A, Beccari T, Saftig P, von Figura K. Efficacy of enzyme replacement therapy in alpha-mannosidosis mice: a preclinical animal study. Hum. Mol. Genet. 2004; 13:1979–1988. [PubMed: 15269179]

14. Matzner U, Herbst E, Hedayati KK, Lüllmann-Rauch R, Wessig C, Schröder S, Eistrup C, Möller C, Fogh J, Gieselmann V. Enzyme replacement improves nervous system pathology and function in a mouse model for metachromatic leukodystrophy. Hum. Mol. Genet. 2005; 14:1139–1152. [PubMed: 15772092]
15. Grubb JH, Vogler C, Levy B, Galvin N, Tan Y, Sly WS. Chemically modified beta-glucuronidase crosses blood-brain barrier and clears neuronal storage in murine mucopolysaccharidosis VII. Proc. Natl. Acad. Sci. U.S.A. 2008; 105:2616–2621. [PubMed: 18268347]
16. Sands MS, Vogler C, Kyle JW, Grubb JH, Levy B, Galvin N, Sly WS, Birkenmeier EH. Enzyme replacement therapy for murine mucopolysaccharidosis type VII. J. Clin. Invest. 1994; 93:2324–2331. [PubMed: 8200966]
17. Birkenmeier EH, Davisson MT, Beamer WG, Ganschow RE, Vogler CA, Gwynn B, Lyford KA, Maltais LM, Wawrzyniak CJ. Murine mucopolysaccharidosis type VII. Characterization of a mouse with beta-glucuronidase deficiency. J. Clin. Invest. 1989; 83:1258–1266. [PubMed: 2495302]
18. Grubb JH, Vogler C, Tan Y, Shah GN, MacRae AF, Sly WS. Infused Fc-tagged beta-glucuronidase crosses the placenta and produces clearance of storage in utero in mucopolysaccharidosis VII mice. Proc Natl. Acad. Sci. U.S.A. 2008; 105:8375–8380. [PubMed: 18544647]
19. Montaño AM, Oikawa H, Tomatsu S, Nishioka T, Vogler C, Gutierrez MA, Oguma T, Tan Y, Grubb JH, Dung VC, Ohashi A, Miyamoto K, Orii T, Yoneda Y, Sly WS. Acidic amino acid tag enhances response to enzyme replacement in mucopolysaccharidosis type VII mice. Mol. Genet. Metab. 2008; 94:178–189. [PubMed: 18359257]
20. Grubb JH, Vogler C, Sly WS. New strategies for enzyme replacement therapy for lysosomal storage diseases. Rejuvenation Res. 2010; 13:229–236. [PubMed: 20345279]
21. Nazarian A, Snyder BD, Zurakowski D, Muller R. Quantitative micro-computed tomotraphy: A non-invasive method to assess equivalent bone mineral density. Bone. 2008; 43:302–311. [PubMed: 18539557]
22. Visigalli I, Delai S, Politi LS, Di Domenico C, Cerri F, Mrak E, D'Isa R, Ungaro D, Stok M, Sanvito F, Mariani E, Staszewsky L, Godi C, Russo I, Cecere F, Del Carro U, Rubinacci A, Brambilla, Quattrini A, Di Natale P, Ponder KP, Naldini L, Biffi A. Gene therapy augments the efficacy of hematopoietic cell transplantation and fully corrects mucopolysaccharidosis type I phenotype in the mouse model. Blood. 2010; 116:5130–5139. [PubMed: 20847202]
23. Vogler C, Levy B, Galvin N, Lessard M, Soper B, Barker J. Early onset of lysosomal storage disease in a murine model of mucopolysaccharidosis type VII: undegraded substrate accumulates in many tissues in the fetus and very young MPS VII mouse. Pediatr. Dev. Pathol. 2005; 8:453–462. [PubMed: 16222480]
24. Tomatsu S, Montaño AM, Ohashi A, Gutierrez MA, Oikawa H, Oguma T, Dung VC, Nishioka T, Orii T, Sly WS. Enzyme replacement therapy in a murine model of Morquio A syndrome. Hum. Mol. Genet. 2008; 17:815–824. [PubMed: 18056156]
25. Garcia AR, Pan J, Lamsa JC, Muenzer J. The characterization of a murine model of mucopolysaccharidosis II (Hunter syndrome). J. Inherit. Metab. Dis. 2007; 30:924–934. [PubMed: 17876721]
26. Simonaro CM, D'Angelo M, He X, Eliyahu E, Shtraizent N, Haskins ME, Schuchman EH. Mechanism of Glycosaminoglycan-Mediated Bone and Joint Disease. Am. J. Pathol. 2008; 172:112–122. [PubMed: 18079441]
27. Metcalf JA, Zhang Y, Hilton MJ, Long F, Ponder KP. Mechanism of shortened bones in mucopolysaccharidosis VII. Mol. Genet. Metab. 2009; 97:202–211. [PubMed: 19375967]
28. Tomatsu S, Montaño AM, Dung VC, Ohashi A, Oikawa H, Oguma T, Orii T, Barrera L, Sly WS. Enhancement of drug delivery: enzyme-replacement therapy for murine Morquio A syndrome. Mol. Ther. 2010; 18:1094–1102. [PubMed: 20332769]
29. Millán JL, Narisawa S, Lemire I, Loisel TP, Boileau G, Leonard P, Gramatikova S, Terkeltaub R, Camacho NP, McKee MD, Crine P, Whyte MP. Enzyme replacement therapy for murine hypophosphatasia. J. Bone Miner. Res. 2008; 23:777–787. [PubMed: 18086009]

30. Nishioka T, Tomatsu S, Gutierrez MA, Miyamoto K, Trandafirescu GG, Lopez PL, Grubb JH, Kanai R, Kobayashi H, Yamaguchi S, Gottesman GS, Cahill R, Noguchi A, Sly WS. Enhancement of drug delivery to bone: characterization of human tissue-nonspecific alkaline phosphatase tagged with an acidic oligopeptide. Mol. Genet. Metab. 2006; 88:244–255. [PubMed: 16616566]

31. Simonaro CM, Ge Y, Eliyahu E, He X, Jepsen KJ, Schuchman EH. Involvement of the Toll-like receptor 4 pathway and use of TNF-α antagonists for treatment of the mucopolysaccharidoses. PNAS. 2010; 107:222–227. [PubMed: 20018674]

Highlights

- Clearance of storage in bone has been limited due to the avascularity of the growth plate.
- Long circulating enzyme replacement therapy rescues bone pathology.
- Improvement of bone lesions was demonstrated by micro-CT and quantitative histopathological assay.

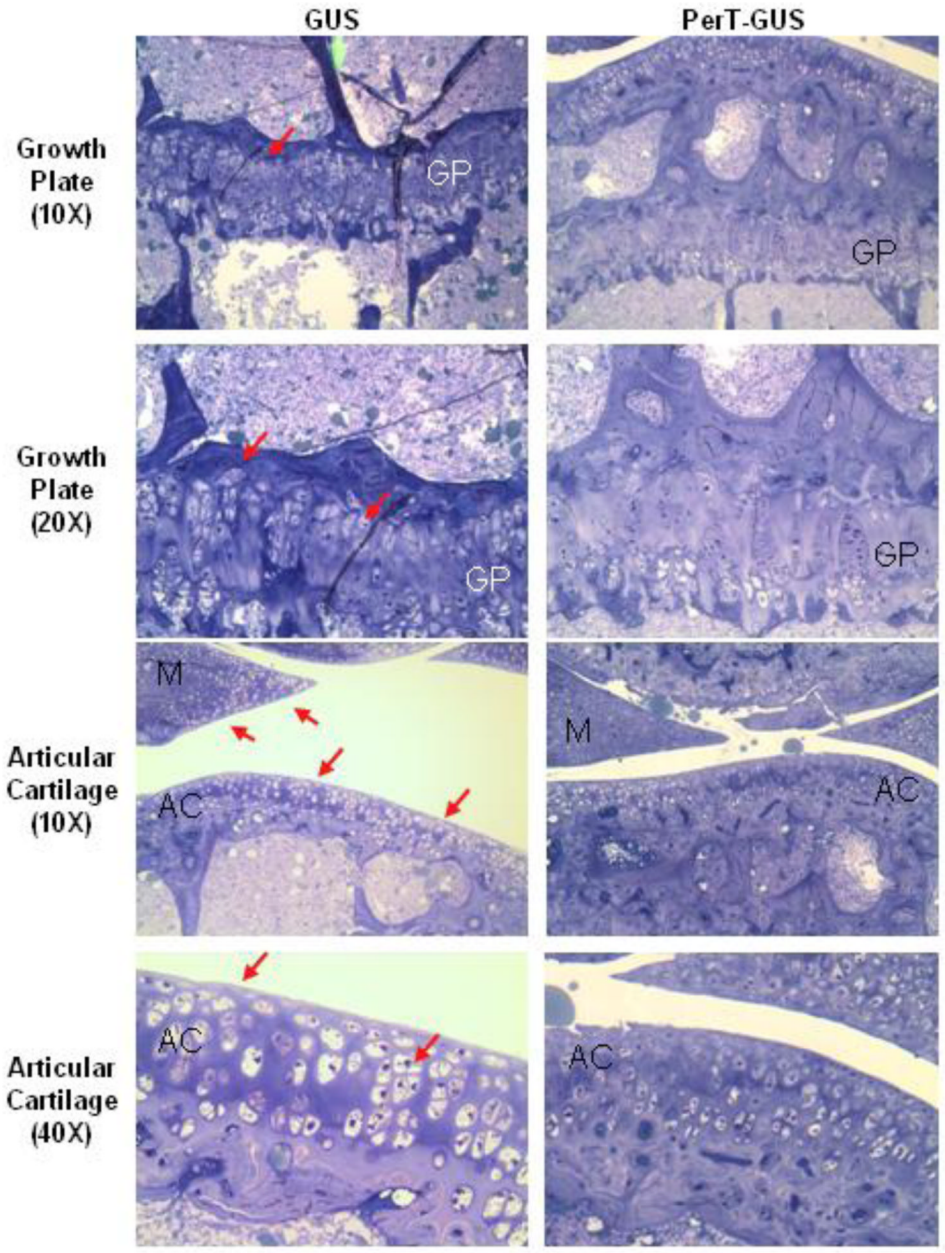

Figure 1.

Histopathology of the knee joint of 17 week-old IV GUS and PerT-GUS treated MPS VII mice. Images are of the growth plate and articular cartilage. Tissue was stained using toluidine blue. PerT-GUS treated mouse shows substantial reduced number of vacuolated cells compared with native GUS treated mouse. Arrows show vacuolated cells in the growth plate, articular cartilage and meniscus area. AC: articular cartilage, GP: growth plate, M: meniscus.

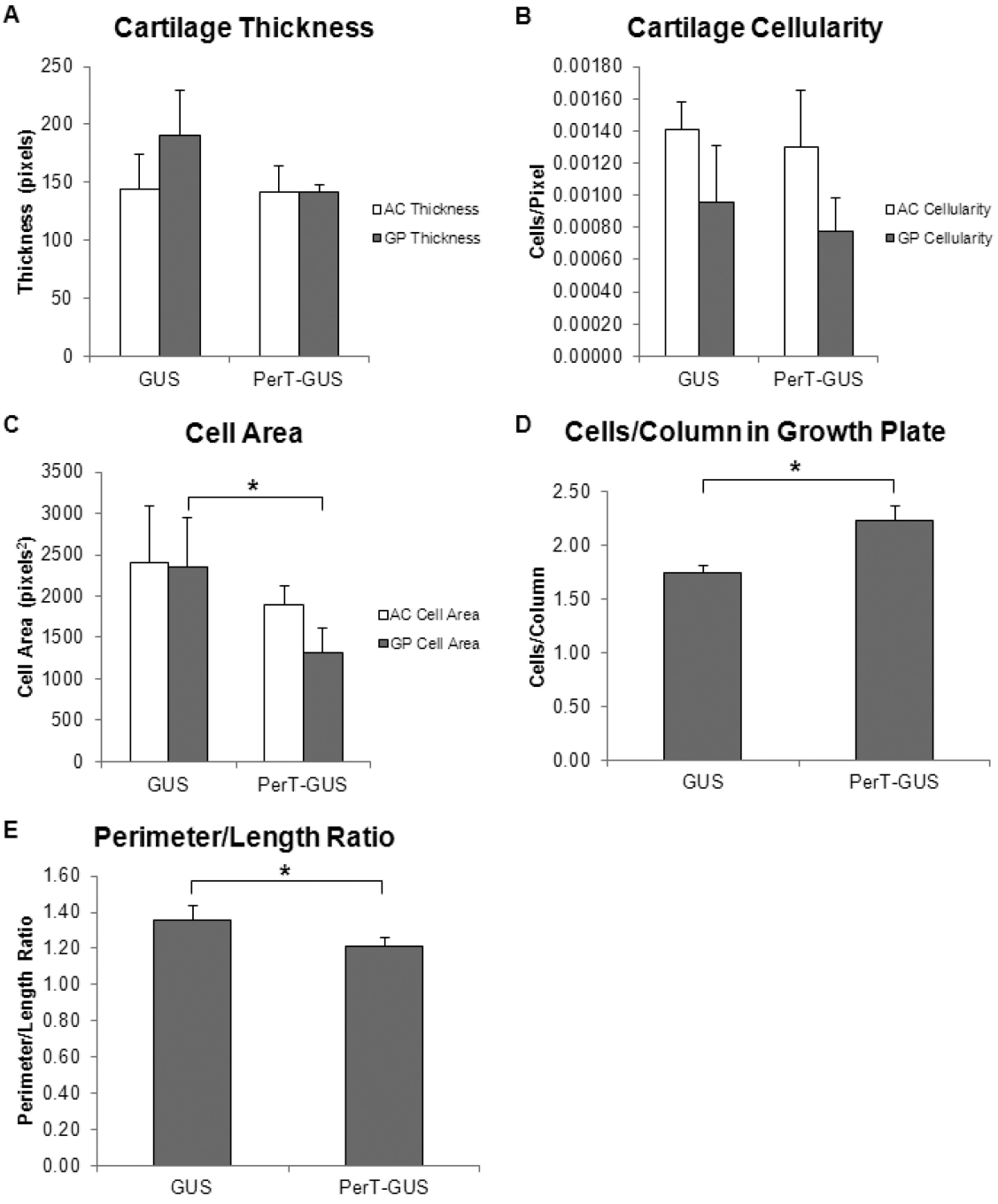

Figure 2.

Quantitative analysis of histopathology of 17 week-old IV GUS (n = 4) and PerT-GUS (n = 4) treated mice. (A) Articular cartilage and growth plate thickness. (B) Articular cartilage and growth plate cellularity (the number of chondrocytes in a given area of the articular cartilage or growth plate). (C) Average cell area of chondrocytes in the proliferative zone of the growth plate and articular cartilage. (D) Mean number of cells per column in the proliferative zone of the growth plate in GUS and PerT-GUS treated mice. (E) The perimeter to length ratio of the growth plate in GUS and PerT-GUS treated mice, this is a measure of the irregularity of the growth plate. * represents $p < 0.05$. AC: articular cartilage, GP: growth plate

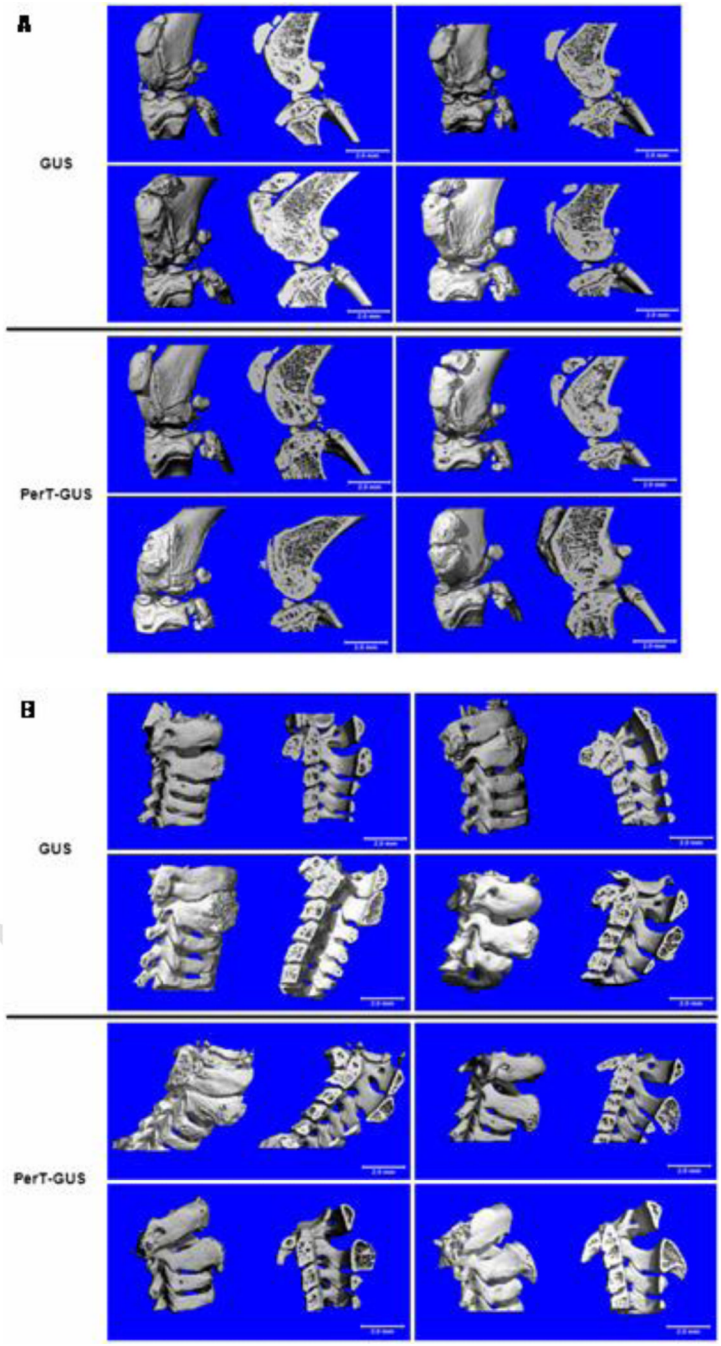

Figure 3.
Micro-CT reconstructions of the knee joints (A) and cervical spines (B) of 17 week-old IV GUS and PerT-GUS treated MPS VII mice. The left side of each picture shows the unsectioned bones, the right side of each picture shows a midline sagittal cross-sections.

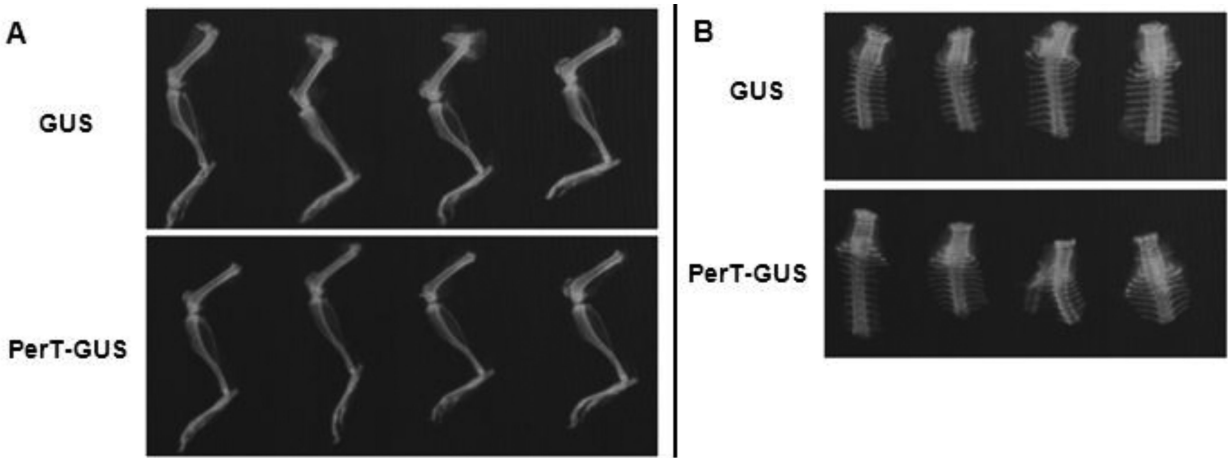

Figure 4.
Radiographs of the legs (A) and spine (B) of 17 week-old IV GUS and PerT-GUS treated mice.

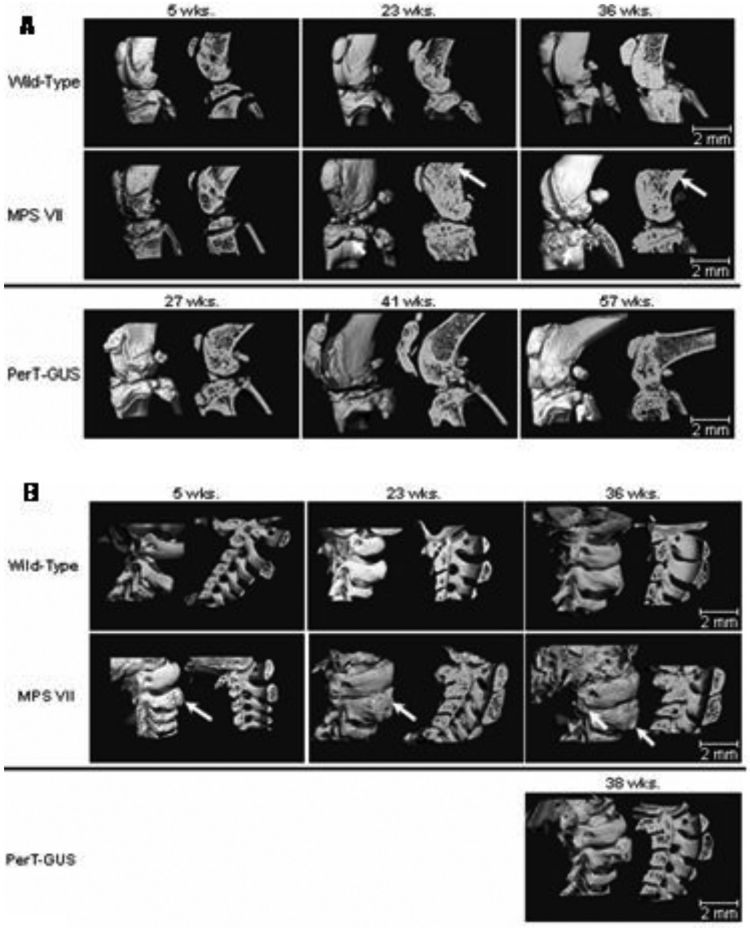

Figure 5.

Three dimensional micro-CT reconstructions of knee joints and spines of wild-type, untreated MPS VII, and IP PerT-GUS treated MPS VII mice. Each picture shows unsectioned bone (left side) or sagittal-sectioned bone (right side). Cross sections are sagittal through the midlines.

A.) The long arrows identify areas of thickened cortical bone. The short arrows identify abnormal exophytic bone formations on articular surfaces. Ages of wild-type and untreated MPS VII mice are 5, 23, and 36 weeks old. Ages of 2 mg/kg PerT-GUS treated mice are 27, 41, and 57 weeks-old.

B.) The arrow on the 5-week-old MPS VII spine identifies an area of decreased bone formation. Arrows on 23- and 36-week-old MPS VII mice identify areas of extra bone formation. Wild-type and MPS VII mice ages are 5, 23, and 36 weeks old. The mouse age treated with 2 mg/kg PerT-GUS is 38 weeks old.

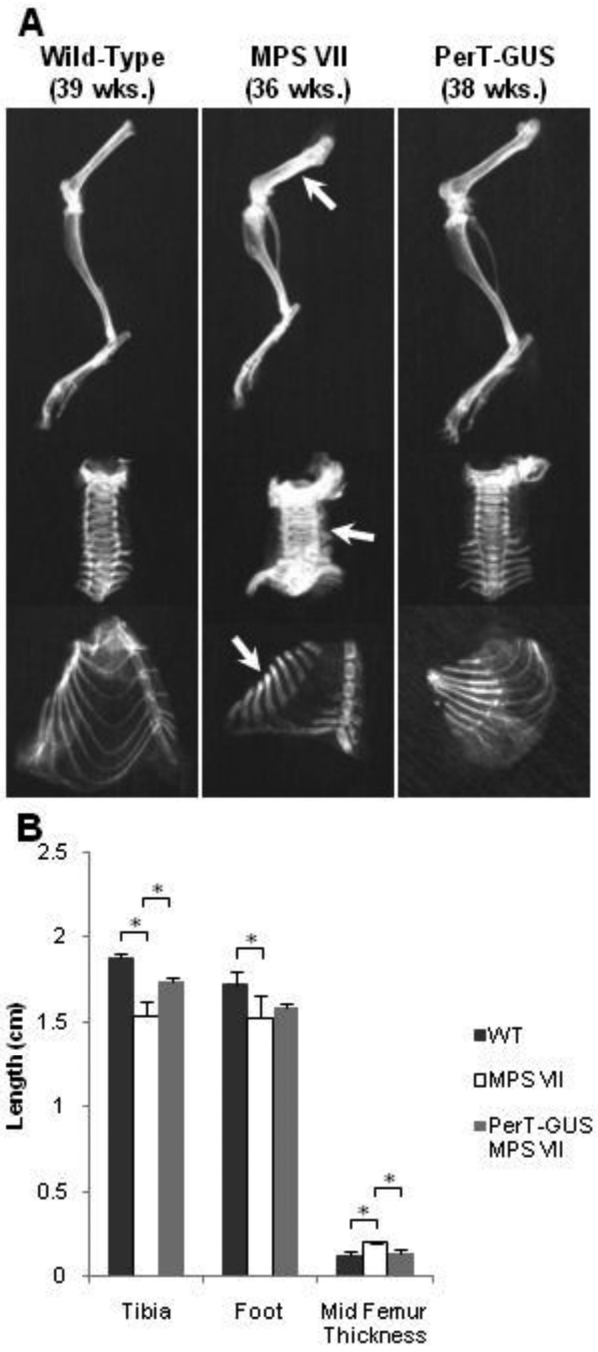

Figure 6.

Radiographs of wild-type, untreated MPS VII, and IP PerT-GUS treated MPS VII mice.

A. Radiographs of legs, spine, and ribcages. Arrows identify areas of bone thickening and increased radiodensity in the femur, cervical spine, and ribs.

B. Leg measurements in X-ray pictures. Values are means (wild-type, n = 5; MPS VII, n = 4; PerT-GUS treated MPS VII, n = 3) with error bars representing one standard deviation.

*significantly decreased compared with wild-type

**significantly decreased compared with untreated MPS VII mice. See Supplemental Fig. 2 for measurement details.

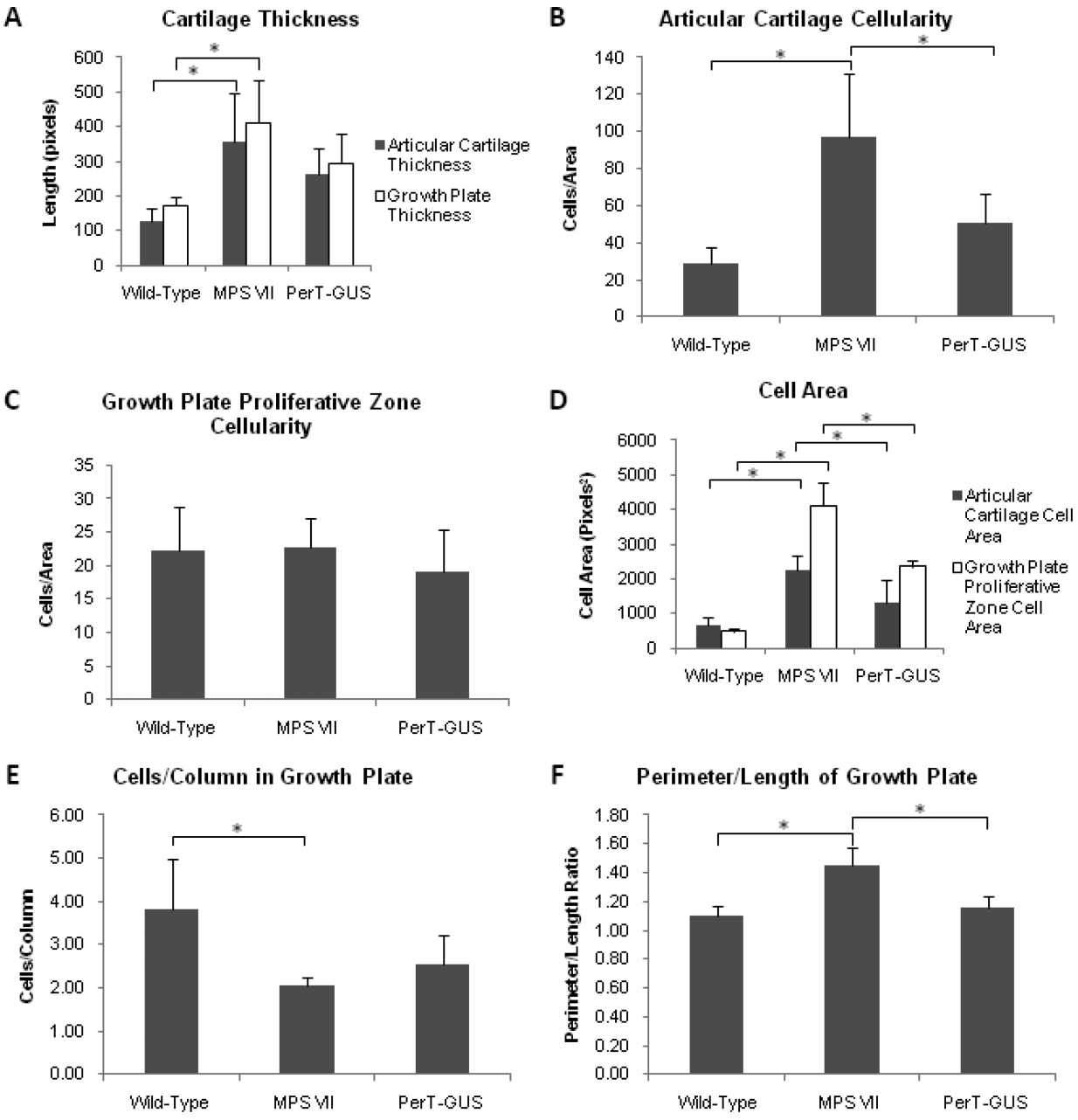

Figure 7.

Histopathology of wild-type (36 weeks old), untreated MPS VII (32 weeks old), and IP PerT-GUS treated MPS VII mice (27 weeks old). Images are of the growth plate, articular cartilage, trabecular bone/bone marrow, and cortical bone. Tissue was stained with toluidine blue. Arrows on growth plate and articular cartilage micrographs identify distended chondrocytes. Arrows on cortical bone micrographs identify distended osteocytes, which are more prevalent in untreated MPS VII bone than in PerT-GUS treated MPS VII bone. GP: growth plate, BM: bone marrow, M: meniscus, AC: articular cartilage.

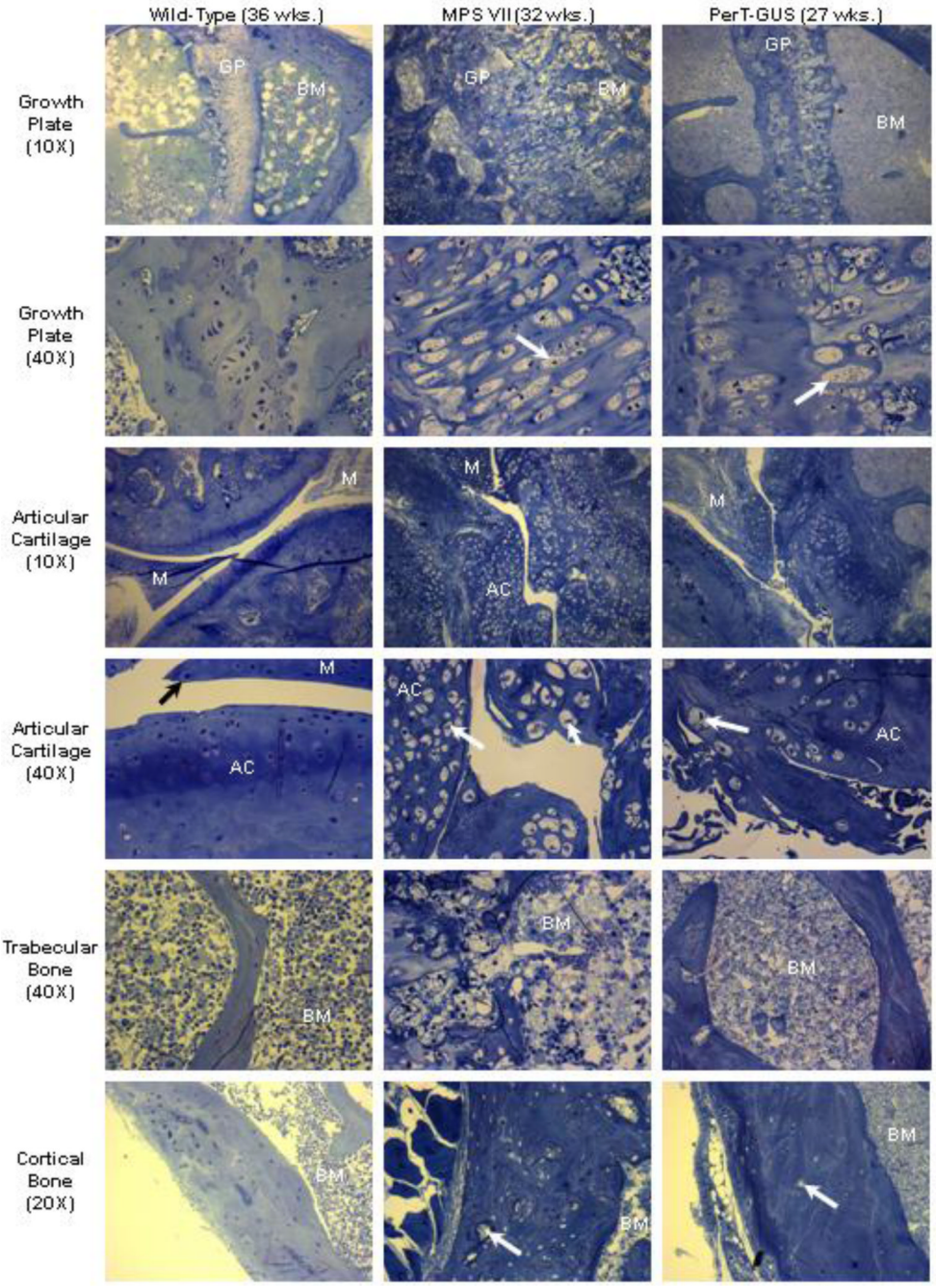

Figure 8.

Quantitative analysis of histopathology of tibias in wild-type (n = 5), untreated MPS VII (n = 4), and IP PerT-GUS treated MPS VII mice (n = 5). (A) Shows growth plate and articular cartilage thickness. (B) Number of chondrocytes in a given area of the articular cartilage (cellularity). (C) Number of chondrocytes in a given area of the proliferative zone of the growth plate (cellularity). (D) Cross sectional cell area of chondrocytes in the proliferative zone of the growth plate or articular cartilage, values reported are means of measurements taken for all chondrocytes in one 40X microscope field. (E) Number of cells in each proliferative zone column in the growth plate. Values reported are means of the number of cells in each column in one 40X microscope field. (F) Perimeter to length ratio measured as

shown in Supplemental Fig. 4. * represents $p < 0.05$. Error bars represent one standard deviation.